lax of the sources or phase changes associated with the instrument *selectively* occurring for one source. However, any such variation must also mimic the phase change due to the gravitational deflection which is antisymmetric with respect to the occultation of 0116+08 near the middle of the experiment. Otherwise, these phase distortions would be readily apparent in the post-fit residual data and included in the error estimate anyway.

A systematic effect associated with the orientation in the sky of the three sources is unlikely since the signals from all of the sources were significantly deflected in a variety of directions during the course of the experiment. A significant departure of the gravitational bending from the expected angular dependence would also lead to large, inexplicable post-reduction residuals.

The measured gravitational deflection determined from the 1974 and 1975 NRAO experiments is $\gamma' = 1.007 \pm 0.009$ (standard error). This corresponds to a value of the parametrized post-Newtonian parameter[2] $\gamma = 1.014 \pm 0.018$ and a deflection at the solar limbs of 1.761 ± 0.016 arc sec. The experiment places significant limits on the scalar coupling constant ω of the Brans-Dicke[3] theory as shown in Table II. With these limits the differences between general relativity and the Brans-Dicke theory of gravitation are slight for most astrophysical applications.

Increased accuracy of the radio deflection experiment can be obtained by using longer baselines. However, even with intercontinental baselines, an improvement by a factor of 5 or 10 may be difficult. Other accurate tests of general relativity, especially those associated with bound orbits, are extremely important since these tests can measure parametrized post-Newtonian parameters other than γ. The deflection experiment can exclude a subset of possible metric gravitational theories.

TABLE II. Limits to the scalar coupling parameter ω.

Probability[a] \ Parameter	γ'	ω
99.9%	>0.97	>15
99 %	>0.98	>23
90 %	>0.99	>35

[a] Based on curves in Fig. 3.

*Operated by Associated Universities, Inc., under contract with the National Science Foundation.

[1] E. B. Fomalont and R. A. Sramek, Astrophys. J. 199, 749 (1975).
[2] C. W. Misner, K. S. Thorne, and J. A. Wheller, *Gravitation* (Freeman, San Francisco, 1973).
[3] R. H. Dicke, Astrophys. J. 152, 1 (1968).

Further Data on the High-y Anomaly in Inelastic Antineutrino Scattering*

A. Benvenuti, D. Cline, W. T. Ford, R. Imlay,† T. Y. Ling, A. K. Mann, D. D. Reeder, C. Rubbia, R. Stefanski, L. Sulak, and P. Wanderer‡

Department Of Physics, Harvard University, Cambridge, Massachusetts 02138, and Department of Physics, University of Pennsylvania, Philadelphia, Pennsylvania 19174, and Department of Physics, University of Wisconsin, Madison, Wisconsin 53706, and Fermi National Accelerator Laboratory, Batavia, Illinois 60510

(Received 23 February 1976)

The high-y anomaly in inelastic $\bar{\nu}_\mu$-nucleon scattering is shown to exhibit effective violations of scale invariance and charge-symmetry invariance. The anomaly cannot be explained by scattering from antiquarks in the usual three-quark model.

Earlier, we presented data on high-energy inelastic ν_μ- and $\bar{\nu}_\mu$-nucleon collisions leading to a single final-state muon which were not readily understood on the basis of present knowledge of semileptonic weak processes at lower energy.[1,2] The $\bar{\nu}$ data showed a significant departure from the expected inelasticity distribution[1]—since called the high-y anomaly after the Bjorken scaling variable $y = (E_{\bar{\nu}} - E_\mu)/E_{\bar{\nu}}$—and exhibited an energy threshold for this effect. This result strongly suggested new-particle production by $\bar{\nu}$; it provided no evidence for or against new-particle production by ν.

We also reported additional stronger evidence for new-particle production in both ν and $\bar{\nu}$ interactions consisting of events in which two muons (dimuons) were observed in the final state.[3-5] The dimuons showed an effective energy threshold similar to that observed in the $\bar{\nu}$ single-muon data. A likely common explanation of both single-muon and dimuon data is the production of one or more massive, short-lived, new hadrons that decay weakly and therefore carry a new quantum number.[2,4-7]

In the present paper we utilize samples of 4994 ν and 2408 $\bar{\nu}$ single-muon events—10 times the initial samples—to extend the search for energy-dependent anomalous distributions. These large numbers of events, in conjunction with better understanding of the experimental resolution and detection efficiency, permit us to measure (i) the y distributions for ν and $\bar{\nu}$ at average energies above 100 GeV, and (ii) the detailed energy dependence of the first moments of the y distributions of ν and $\bar{\nu}$ in the region 10 to 150 GeV. The higher-energy data show effective violations of scale invariance and charge-symmetry invariance that cannot be explained by the apparent antiquark content (of the conventional three-quark model) that is specified by the lower-energy data.

The details of the experimental apparatus and the measured resolution in E_H and E_μ were described previously.[8,9] Using those directly measured resolution functions, we have constructed in a Monte Carlo calculation the pattern of migration of events in the x-y plane due to resolution smearing. Here $x = Q^2/2mE_H$, where $Q^2 = 4E_\nu E_\mu \times \sin^2(\theta_\mu/2)$, $E_\nu = E_\mu + E_H$, and m is the nucleon mass. The calculated patterns for $\bar{\nu}$ show negligible migration of events from low y—where the density is greatest—to high y. There is a systematic migration, as expected from the measured x resolution, from low x to high x that is largely independent of y. Migration patterns that have been constructed for different trial distributions, different energy intervals, different regions of x, and with variations of the resolution function all show similar behavior, and lead to the unequivocal conclusion that resolution smearing is not the source of the observed high-y anomaly.

In Fig. 1 are shown the calculated approximate limits on the *geometric* detection efficiency of the apparatus in the Bjorken x-y space for different ν, $\bar{\nu}$ energies. The limits satisfy the requirement that, in any x bin, the integrated efficiency in y below the limit is 0.8. Using the information represented by Fig. 1 we have applied a weighting factor (ϵ_μ^{-1}) to each observed event to take into account the detection efficiency in a model-independent fashion. *No correction has been applied to the data for unobserved events outside the angular acceptance or muon range cutoff of the apparatus.* Nor have the data been corrected for resolution smearing. In the y distributions shown below, however, we have integrated only over the interval $x \leq 0.60$ to avoid the region of poor resolution and poor detection efficiency at $x > 0.60$. Our conclusions are not dependent on that x cut.

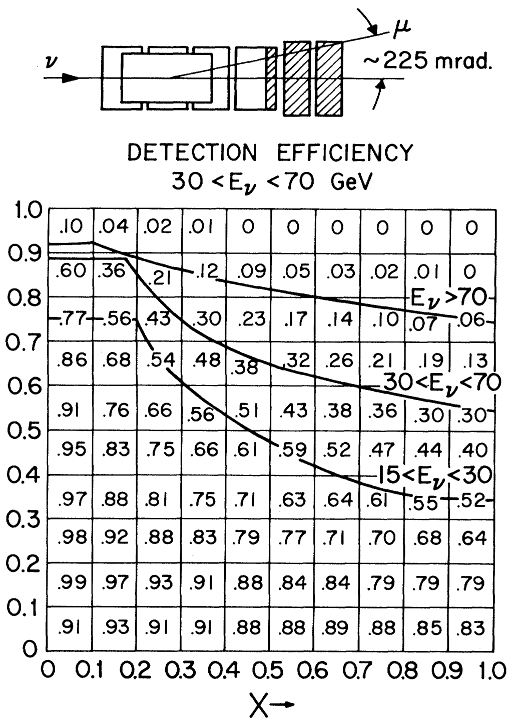

FIG. 1. Dectection efficiency ϵ_μ of the apparatus. The solid lines are geometric limits determined exclusively by the angular acceptance of the muon magnetic spectrometer, and by ranging out of muons with energies less than 4 GeV. The numerical values of ϵ_μ correspond to the (sample) energy interval $30 < E_{\nu,\bar{\nu}} < 70$ GeV.

About $\frac{1}{2}$ of the ν sample and $\frac{2}{3}$ of the $\bar{\nu}$ sample were obtained simultaneously with mixed ν and $\bar{\nu}$ beams formed by magnetic horn focusing of the secondary mesons that decay in flight to yield the ν and $\bar{\nu}$. The remainders of the ν and $\bar{\nu}$ samples were acquired with quadrupole magnet focusing, which yields appreciably hardened ν and $\bar{\nu}$ spectra compared to the magnetic-horn-focused spectra. It is of particular importance that the distributions in x and y obtained with these quite different beam types are essentially identical because it indicates that neither the experimental detection efficiency nor the experimental resolution depended in any unexpected way on the nature of the incident ν, $\bar{\nu}$ beams.

Figures 2(a) and 2(b) show the distributions in y for ν and $\bar{\nu}$ with $10 < E_{\nu,\bar{\nu}} \leq 30$ GeV. The y^{ν} distribution is approximately uniform out to $y = 0.6$ where the restricted angular acceptance and range cutoff terminate the distribution (see Fig. 1). The $y^{\bar{\nu}}$ distribution, on the other hand, falls rapidly with increasing y in the same y region. These distributions are consistent with the forms expected from the scale-invariant differential cross sections for inclusive ν and $\bar{\nu}$ scattering,

$$(d\sigma/dy)^{\nu} = (G^2 M E_{\nu}/\pi)\int F_2(x)\, dx[1 - y(1 - B^{\nu}) + \tfrac{1}{2}y^2(1 - B^{\nu}) + \tfrac{1}{2}y^2 R_L{}^{\nu}] \qquad (1)$$

and

$$(d\sigma/dy)^{\bar{\nu}} = (G^2 M E_{\bar{\nu}}/\pi)\int \bar{F}_2(x)\, dx[1 - y(1 + B^{\bar{\nu}}) + \tfrac{1}{2}y^2(1 + B^{\bar{\nu}}) + \tfrac{1}{2}y^2 R_L{}^{\bar{\nu}}], \qquad (2)$$

with

$$B^{\nu} = -\int xF_3(x)\, dx \Big/ \int F_2(x)\, dx, \quad B^{\bar{\nu}} = -\int x\bar{F}_3(x)\, dx \Big/ \int \bar{F}_2(x)\, dx,$$

and

$$R_L{}^{\nu} = \int [2xF_1(x) - F_2(x)]\, dx \Big/ \int F_2(x)\, dx, \quad R_L{}^{\bar{\nu}} = \int [2x\bar{F}_2(x) - \bar{F}_1(x)] \Big/ \int \bar{F}_2(x)\, dx,$$

where the $F_i(x)$ are dimensionless, scale-invariant, nucleon structure functions. Fitting to the data of Figs. 2(a) and 2(b) yields $B^{\nu} = 0.60 \pm 0.30$ and $B^{\bar{\nu}} = 0.94 \pm 0.09$ in the region $x < 0.6$ if $R_L{}^{\nu}$ and $R_L{}^{\bar{\nu}}$ are taken to be zero.

Figures 3(a) and 3(b) show the corresponding y^{ν} and $y^{\bar{\nu}}$ distributions in the energy region $E_{\nu,\bar{\nu}} > 70$ GeV. Here the y^{ν} distribution is fitted by $B^{\nu} = 0.83 \pm 0.20$ out to the cutoff in detection efficiency at $y = 0.85$. In contrast, the $y^{\bar{\nu}}$ distribution in Fig. 3(b) is best fitted by $B^{\bar{\nu}} = 0.41 \pm 0.13$. This is the

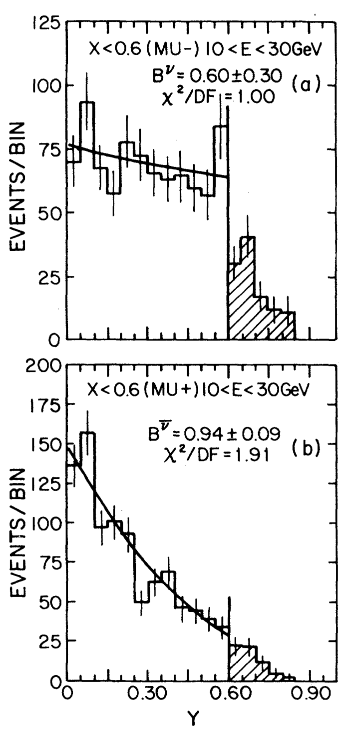

FIG. 2. Distributions in y for (a) 946 ν events and (b) 991 $\bar{\nu}$ events with $10 < E_{\nu,\bar{\nu}} < 30$ GeV. The cross-hatched areas are in a y region in which the correction for detection efficiency is incomplete (Fig. 1); they are not included in the fits for $B^{\nu,\bar{\nu}}$.

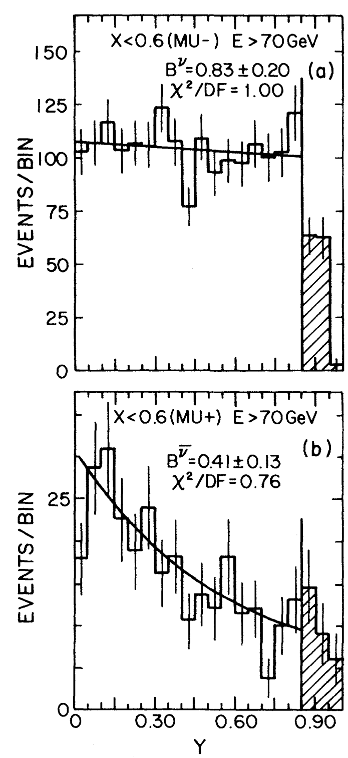

FIG. 3. Distributions in y for (a) 1905 ν events with $\langle E_{\nu}\rangle = 126$ GeV, and (b) 310 $\bar{\nu}$ events with $\langle E_{\bar{\nu}}\rangle = 106$ GeV. The cross-hatched areas mean the same as in Fig. 2, but note the improvement in detection efficiency with energy.

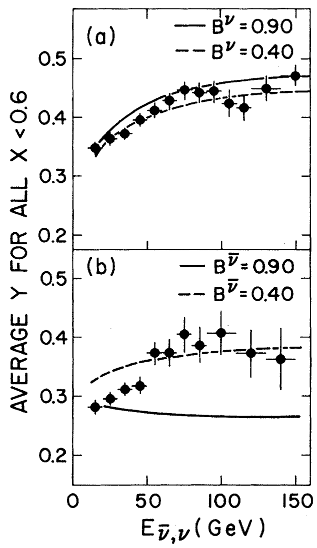

FIG. 4. First moments of the y distributions versus energy for (a) ν events and (b) $\bar{\nu}$ events.

most direct manifestation in the data of the high-y anomaly: The form of the y^{ν} distribution remains constant with energy, while the form of the $y^{\bar{\nu}}$ distribution changes with energy.

To explore further the energy dependence of the y distributions we plot in Figs. 4(a) and 4(b) the first moments $\langle y^{\nu}\rangle$ and $\langle y^{\bar{\nu}}\rangle$ (for all $x<0.6$) as functions of E_{ν} and $E_{\bar{\nu}}$. At energies less than about 70 GeV $\langle y^{\nu}\rangle$ is too small because of the loss of events at high y (Fig. 1). We have taken that loss into account in the Monte Carlo calculations of $\langle y^{\nu}\rangle$ with which the data in Fig. 4(a) are compared. Because of lack of sensitivity, the experimental measurements of $\langle y^{\nu}\rangle$ in the energy interval 15 to 150 GeV do not determine a precise value of the parameter B^{ν}, as shown earlier by the y^{ν} distributions in Figs. 2(a) and 3(a). However, the data for $\langle y^{\bar{\nu}}\rangle$, which correspond to $B^{\bar{\nu}}=0.9$ at $E_{\bar{\nu}}<30$ GeV, rise sharply to a significantly higher value of $\langle y^{\bar{\nu}}\rangle$ at higher $E_{\bar{\nu}}$. There is no single value of $B^{\bar{\nu}}$ which satisfactorily describes the dependence of $\langle y^{\bar{\nu}}\rangle$ on $E_{\bar{\nu}}$ over the entire energy range of Fig. 4(b). This is shown by comparison with the Monte Carlo calculated curves for two values of $B^{\bar{\nu}}$ in Fig. 4(b). No energy-dependent misbehavior of the experimental apparatus is known to us that would introduce a spurious energy threshold in $\langle y^{\bar{\nu}}\rangle$ in the vicinity of 30 GeV, leading them to such large values of $\langle y^{\bar{\nu}}\rangle$.

There remains still the question of alternative possible explanations of the high-y anomaly. In particular, in the quark-parton model with three quarks (u, d, and s), scattering from antiquarks is expected to contribute a uniform component to the $y^{\bar{\nu}}$ distribution and a $(1-y)^2$ component to the y^{ν} distribution. Within the context of the quark-parton model, however, we can directly evaluate the fraction of antiquarks necessary to explain the high-y anomaly from the anomaly itself. The parameter $B^{\bar{\nu}}$ in Eq. (2) is related to the fraction of antiquarks by the equation

$$B^{\bar{\nu}} \equiv -\int x\bar{F}_3(x)\,dx \Big/ \int \bar{F}_2(x)\,dx = 1 - 2\int \bar{q}(x)\,dx \Big/ \int [\bar{q}(x)+q(x)]\,dx, \qquad (3)$$

where $q(x)$ and $\bar{q}(x)$ are the momenta in the nonstrange quarks and antiquarks. Accordingly, the curves marked $B^{\bar{\nu}}=0.90$ and $B^{\bar{\nu}}=0.40$ in Fig. 4 correspond to $\int \bar{q}(x)\,dx/\int[\bar{q}(x)+q(x)]\,dx=0.05$ and 0.30, respectively. Low-energy $\bar{\nu}$ data[10] are consistent with $\int\bar{q}(x)\,dx/\int[\bar{q}(x)+q(x)]\,dx=0.09\pm0.04$, and recent muon-nucleon scattering data[11] yield, in the same context, a value less than 0.10; the data for $E_{\bar{\nu}}<30$ GeV of this Letter give 0.05 ± 0.05. We conclude that $\bar{\nu}$ scattering from the antiquarks of the conventional three-quark model is unable to account for the observed energy threshold and is too small to account for the magnitude of the high-y anomaly.

In summary, the high-y anomaly in inelastic $\bar{\nu}_{\mu}$-nucleon scattering has been verified. No direct manifestation of a high-y anomaly is present in the ν_{μ} data. Taken together, the ν and $\bar{\nu}$ data show effective violations of both scale invariance and charge-symmetry invariance; this supports the hypothesis of new-particle production as the common explanation of the high-y anomaly and ν- and $\bar{\nu}$-induced dimuons.

*Work supported in part by the U. S. Energy Research and Development Administration.

†Now at Rutgers University, New Brunswick, N. J. 08903.

‡Now at Brookhaven National Laboratory, Upton, N. Y. 11973.

[1]A. Benvenuti *et al.*, Phys. Rev. Lett. 33, 984 (1974).

[2]A. Benvenuti *et al.*, Phys. Rev. Lett. 34, 597 (1975).

[3]A. Benvenuti *et al.*, Phys. Rev. Lett. 34, 419 (1975).

[4]A. Benvenuti *et al.*, Phys. Rev. Lett. 35, 1199, 1203 (1975).

[5]A. Benvenuti *et al.*, Phys. Rev. Lett. 35, 1249 (1975).

[6]See, for example, L. N. Chang, E. Derman, and J. Ng, Phys. Rev. Lett. 35, 6 (1975).

[7]A. Pais and S. B. Treiman, Phys. Rev. Lett. 35, 1206 (1975).

[8]A. Benvenuti *et al.*, Nucl. Instrum. Methods 125, 447

(1975).
[9]A. Benvenuti *et al.*, Nucl. Instrum. Methods 125, 457 (1975).
[10]H. Deden *et al.*, Nucl. Phys. B85, 269 (1975).
[11]L. Mo, in *Proceedings of the International Symposium on Lepton and Photon Interactions at High Energy, Stanford, California, 1975*, edited by W. T. Kirk (Stanford Linear Accelerator Center, Stanford, Calif., 1975).

Observation of a Peak in the $\bar{K}^0\pi^+\pi^-$ Effective Mass at 1700 MeV

A. Etkin, K. J. Foley, J. H. Goldman, W. A. Love, T. W. Morris, S. Ozaki, E. D. Platner, A. C. Saulys, C. D. Wheeler, and E. H. Willen
Brookhaven National Laboratory, Upton, New York 11973*

and

S. J. Lindenbaum
Brookhaven National Laboratory, Upton, New York 11973, and City College of The City University of New York,† New York, New York 10031*

and

I.-J. Kim, M. A. Kramer, and U. Mallik
City College of The City University of New York,† New York, New York 10031
(Received 4 May 1976)

We have investigated the reaction $K^-p \to \bar{K}^0\pi^+\pi^-n$ with 6 GeV/c K^-. We observe a statistically significant (6.6 standard deviations) peak in the $\bar{K}^0\pi^+\pi^-$ effective mass at 1692 ± 6 MeV with a full width $\Gamma = 26^{+24}_{-17}$ MeV.

We report a study of the reaction $K^-p \to \bar{K}^0\pi^+\pi^-n$ at 6 GeV/c, in which we observe a peak in the $\bar{K}^0\pi^+\pi^-$ mass spectrum suggesting a new resonance at 1700 MeV. The charge-exchange channel was chosen in order to avoid the background problems common to diffractive channels. The experiment was performed at the Brookhaven National Laboratory alternating gradient synchrotron with a partially separated K^- beam at an incident momentum of 6 GeV/c. The pion-to-kaon ratio in the beam was typically 4:1. The effective pion contamination was reduced to less than 1% using two threshold Cherenkov counters. The detection apparatus was the Brookhaven National Laboratory multiparticle spectrometer[1] (see Fig. 1). A 51-cm-long liquid-hydrogen target positioned in the 10-kG magnetic field was followed by a downstream detection system comprising 42 planes of magnetostrictive spark chambers. Two planar proportional wire chambers (PWC) were used in the trigger, one immediately downstream of the target (TPX1) and another in between spark-chamber modules, 56 cm further downstream (TPX2). The trigger demanded 2–4 charged particles in the central 40 cm of TPX1 and 4–6 charged particles in TPX2; thus the K_s^0 could decay into $\pi^+\pi^-$ anywhere between the production vertex and TPX2 and still trigger the apparatus (the relatively loose trigger requirement in TPX2 reduced the loss of data due to δ rays, etc.). In addition an open-ended rectangular box of scintillation counters, 38 cm wide by 38 cm high by 96 cm long, surrounding the target was used to veto events with charged recoil particles; for approximately 30% of the data the box was lined with 3 mm of lead to provide a π^0 veto.

The events were reconstructed by a computer program which first identified and fitted individual tracks. These tracks were then extrapolated

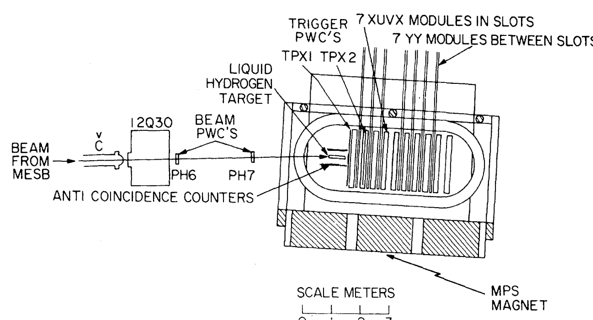

FIG. 1. Plan view of those parts of the multiparticle spectrometer used for this experiment. The devices labeled YY and $XUVX$ are multiple-gap wire spark chambers with magnetostrictive readout.